Communications in Physics, Vol. 27, No. 2 (2017), pp. 97-106
DOI:10.15625/0868-3166/27/2/9217

Invited Paper

PERTURBATIVE NONLINEAR OPTICS IN THE EXTREME ULTRAVIOLET REGION

LAP VAN DAO† AND PETER HANNAFORD

Centre for Quantum and Optical Science, Faculty of Science Engineering and Technology, Swinburne University of Technology, Melbourne, Australia 3122

†*E-mail:* dvlap@swin.edu.au

Received 13 February 2017
Accepted for publication 12 May 2017
Published 30 June 2017

Abstract. *We report the investigation of the wave-mixing process with two multiple-cycle pulses having incommensurate frequencies (at 1400 nm and 800 nm). With a collinear and non-collinear configuration of the two beams, a different extreme ultraviolet (XUV) mixing field can be created at low intensity of the 800 nm field. For a high intensity of the second laser pulse we are able to amplify the XUV radiation. We show that the dynamics of the free electrons can be revealed from the frequency mixing process.*

Keywords: laser applications, nonlinear optics, high-order harmonic generation.

Classification numbers: 42.55.-f, 42.65.-k, 42.62.Fi.

I. INTRODUCTION

Information on energy levels, transition dipole moments, and electronic and nuclear motions in atoms and molecules can be obtained from linear spectroscopy or one-dimensional spectroscopy where the signals are recorded versus a single time or frequency parameter. It is well known that in the visible and infrared range the dynamics of the microscopic structure of matter interacting with a strong laser field departs from the perturbative approach [1], in which the response of the medium is expanded in many orders, expressed as linear and nonlinear terms. The low-order response of a material to a laser field, e.g., third or fifth order, has been used to study structures of matter and their dynamics. Four-wave mixing [2] is the most common type of nonlinear spectroscopic technique where a sequence of three pulses interacts with a material to generate a signal which is detected along one of the combinations of the three incoming pulse directions.

The detailed response of a single atom or molecule to an intense electromagnetic field is quite complex, but the fundamental underlying physics can be unexpectedly simple in many cases.

The wave-packet created by a laser field plays a fundamental role in understanding the quantum picture and provides a bridge between the quantum picture and the classical concept of the trajectory of a particle [3, 4]. The motion of the wave-packet reflects the time evolution of a coherent superposition of the system. Useful information regarding the discrimination and visualization of the wave-packet dynamics can be obtained from time-resolved photoelectron imaging because of the sensitivity of the photoelectron angular distribution to the electronic symmetry.

The high-order harmonic generation process provides methods to produce very short pulses (attosecond pulses) of coherent radiation in the extreme ultraviolet and soft X-ray region. This source opens up new applications such as in time-resolved studies of atoms and molecules [5, and references therein], and coherent diffractive imaging [6]. Soft X-ray light sources will provide new nonlinear spectroscopic tools that can be used to reveal core-level electronic resonances and their interactions, and permit the creation of non-stationary electronic wave-packets and monitoring their dynamics. At these frequencies and timescales, experimental techniques are generally sensitive to electronic coherences.

The dynamics of the excited wave-packet can be studied by using of a second, off-axis, long-pulse, laser beam to control the HHG process [7]. Bertrand *et al.* [8] have shown that when two intense fundamental laser pulses of frequency ω and 2ω are crossed non-collinearly in a gas-jet target the emission spectrum can be described simply in terms of conservation of energy and momentum. We have realised optical wave-mixing [9] and amplification [10] in HHG which suggests the possibility to treat the physics in the XUV range with a perturbative nonlinear optics theory.

In this paper we review the wave-mixing process by using two multiple-cycle pulses with incommensurate frequencies (at 1400 nm and 800 nm). With a collinear and non-collinear configuration of the two beams, different extreme ultraviolet mixing fields can be created and separated spatially and spectrally. We consider the wave mixing and application of extreme ultraviolet radiation with a perturbative nonlinear optics approach. We show that the time evolution of mixing field can be used for studies of the coherence time of the free electron wave-packet.

II. THEORETICAL BACKGROUND

The slowly varying envelope amplitude $A_i(z,t)$ for the driving laser field $E_1(z,t)$ and for the generated field $E_2(z,t)$propagating along the z-direction is given by

$$E_1(z,t) = \frac{1}{2}A_1(z,t)\,e^{i(k_1 z-\omega_1 t)} + c.c. \tag{1}$$

$$E_2(z,t) = \frac{1}{2}A_2(z,t)\,e^{i(k_2 z-\omega_2 t)} + c.c. \tag{2}$$

where k_1, k_2 are the wave vectors and ω_1, ω_2 are the frequencies of the pump and the generating (new) field, respectively. In this approximation the generation of new fields can be described by [10]

$$\frac{dA_2}{dz} + \frac{\alpha_2}{2}A_2 = i\gamma_2 e^{-i\Delta k_2 z}, \tag{3}$$

where γ_2 is the nonlinear driving term

$$\gamma_2 = \frac{2\pi\omega_2}{cn_2} N d_2^{NL}, \tag{4}$$

α_2 is the absorption coefficient, Δk_2 is the wave-vector mismatch of the driving and generated fields, n_2 is the refractive index, N is the atomic density and d_2^{NL} is the nonlinear response of the medium produced by one or few driving laser fields. In perturbation theory

$$N d_2^{NL} = \frac{\chi^{(q)}}{2^{(q-1)}} A_i^j \tag{5}$$

where $\chi^{(q)}$ is the susceptibility for the q^{th} order process. We assume that the interaction length L is small for considering Δk_2 and $d_2^{NL} \approx$ const. Solving Eq. (5) by integrating over the length of the medium L, we obtain for the intensity of the new field

$$I_2 = \frac{\pi\omega_2^2}{2cn_2} |d_2^{NL}|^2 N^2 L^2 e^{-\omega_2 L/2} \frac{\sin^2\left(\frac{\Delta k_2 L}{2}\right) + \sinh^2\left(\frac{\alpha_2 L}{4}\right)}{\left(\frac{\Delta k_2 L}{2}\right)^2 + \left(\frac{\alpha_2 L}{4}\right)^2} \tag{6}$$

In the case of parametric generation and amplification, the generation and propagation of the idler (i) and signal (s) fields driven by high-order (p) nonlinear response to the pump field A_p can be written [11]

$$\frac{dA_i}{dZ} + \alpha_i A_i = i\frac{\pi\omega_i (q+1)}{cn_i 2^{q-1}} N\chi^{(q+1)}(\omega_i) A_p^q A_s^* e^{(i\Delta kZ)} \tag{7}$$

$$\frac{dA_s}{dZ} + \alpha_s A_s = i\frac{\pi\omega_s (q+1)}{cn_s 2^{q-1}} N\chi^{(q+1)}(\omega_s) A_p^q A_i^* e^{(i\Delta kZ)} \tag{8}$$

where $\Delta k = qk_p - k_s - k_i$ is the wave-vector mismatch, $\chi^{(q+1)}(\omega_i)$ and $\chi^{(q+1)}(\omega_s)$ are the $(q+1)^{th}$ nonlinear susceptibilities, and α_i, α_s is the absorption.The general solutions of Eqs. (6) and (7) are

$$A_i^* = \left\{ -i\frac{\gamma_i^*}{G} A_{s0} \sinh(Gz) + A_{i0}^* \left[\cosh(Gz) + \frac{\beta}{G}\sinh(Gz) \right] \right\} e^{(-\alpha_i z - \beta z)} \tag{9}$$

$$A_s = \left\{ -i\frac{\gamma_s}{G} A_{i0}^* \sinh(Gz) + A_{s0} \left[\cosh(Gz) - \frac{\beta}{G}\sinh(Gz) \right] \right\} e^{(-\alpha_s z + \beta z)} \tag{10}$$

where

$$\gamma_{s,i} = \frac{2\pi\omega_{s,i}}{cn_{s,i}} \frac{(q+1)\chi^{q+1}(\omega_{s,i})}{2^q} N A_p^q \tag{11}$$

$$\beta = \frac{1}{2}(\alpha_s - \alpha_i - i\Delta k) \tag{12}$$

$$G = \sqrt{\beta^2 + \gamma^2}; \gamma^2 = \frac{1}{2}(\gamma_i^* \gamma_s + \gamma_s^* \gamma_i) \tag{13}$$

γ is the nonlinear coupling coefficient between the idler and signal field. The $\gamma_{s,i}$ are determined by the amplitudes of the corresponding nonlinear atomic dipole moments which depend on the intensity of the driving field A_p and the optical properties of the medium. When ω_i is in the visible or infrared regions the absorption by the gas medium is very small or $\alpha_i = 0$ and $\omega_s \gg \omega_i$.

Experiment and theory of high-order harmonic generation show that the intensity of successively higher harmonic orders does not decrease significantly, as is expected in perturbative nonlinear optics. We consider that the non-linear response is constant over a range of high orders. When the pump field with carrier frequency ω_p is very strong ($\geq 10^7$ V/cm) high nonlinear orders of the medium response need to be considered. When $A_{s0} \neq 0$ and $A_{i0} = 0$ are boundary conditions at $z = 0$ the signal field is given by [9,10]

$$A_s = \left\{ A_{s0} \left[\cosh(Gz) - \frac{\beta}{G} \sinh(Gz) \right] \right\} e^{(-\alpha_s z + \beta z)} \tag{14}$$

The intensity of the XUV radiation is then given by

$$I_S = |A_S|^2 \tag{15}$$

Since the nonlinear coupling coefficient γ is small for high-order processes, for the realization of parametric amplification implementation of the phase-matching condition $\Delta k \cong 0$ is an important requirement and is a rather complex problem in the case of high-intensity laser fields. Energy and momentum conservation are given by $q\omega_p = \omega_s + \omega_i$ and $q\boldsymbol{k}_p = \boldsymbol{k}_s + \boldsymbol{k}_i$. The dispersion of the medium leads to a phase-mismatch $\Delta\boldsymbol{k} = (q\boldsymbol{k}_p - \boldsymbol{k}_i) - \boldsymbol{k}_s \cong q\boldsymbol{k}_p - \boldsymbol{k}_s (q \gg 1)$ when the idler field is in the visible or infrared regions. For a collinear configuration of amplification along the propagation direction (z) of the pump field the phase-mismatch without consideration of the phase change of the field around the focus can be written [12]

$$\begin{aligned} \Delta k(z) =& qk_p - k_s \\ =& q \left[N_a (1 - \eta(t)) \frac{2\pi}{\lambda_p} \delta n - \eta(t) N_a r_e \lambda_p \right] + (\text{dipole phase term}) \end{aligned} \tag{16}$$

where λ_p is the centre wavelength of the pump pulse, N_a is the number density of atoms at 1 atmosphere, $\eta(t)$ is the ionization fraction, r_e is the classical electron radius, and δn is the difference between the refractive indices including the nonlinear components at the pump and harmonic wavelengths. The first term in Eq. (16) is related to the dispersion of the neutral medium, which is negative, and the second term is the plasma dispersion, which is positive. The major sources of phase-mismatch are pressure-dependent, which allows the phase-matching condition to be satisfied in plasmas with arbitrary electron density. Full phase-matching can be achieved within a few optical cycles of the laser pulse by eliminating the phase-mismatch.

III. EXPERIMENTS AND RESULTS

III.1. Experiment setup

A 800 nm, 10 mJ, 30 fs, 1 kHz repetition rate laser beam is split into two beams, with pulse energies of 6 mJ and 4 mJ. The 6 mJ beam is used to pump a three-stage optical parametric amplifier (OPA) system to generate an infrared (IR) driving pulse at 1400 nm with energy ~ 2 mJ and duration 40 fs. The 4 mJ (800 nm) pulse or a part (~ 1 mJ) of this pulse is used as an amplifier or mixing field. The IR pulse is used for phase-matched generation of XUV radiation and the 800 nm pulse, which is used to control the HHG output, is aligned in the same direction or at a very small angle to the direction of the IR beam by a dichroic mirror. The polarizations of the two pulses are parallel. The focus position of the two beams can be varied and shifted relative to each other which allows control of the intensity and the spatial profile of the output XUV radiation. The

time delay between the two pulses is controlled by a motorized delay stage with 0.1 fs resolution. Positive delay time implies that the 800 nm pulse precedes the 1400 nm pulse. The laser beams are used to drill an exit pinhole in a thin aluminium plate allowing straight-forward handling, and no further alignment procedure along the optical axis of the 1400 nm pulse is needed. The diameter of the two beams at the focus is $\sim 100\ \mu$m. A long (~ 30 mm) cell filled with argon gas at a pressure of $\sim$250 Torr is used as the interaction medium [13]. The interaction length, where the XUV radiation is generated, is ~ 1 mm and close to the exit pinhole. The harmonic emission enters a flat-field XUV spectrometer comprising a slit, concave grating, and a cooled 14-bit CCD camera. A non-collinear configuration of the two beams helps to spatially separate the wave-mixing field from the 1400 nm and 800 nm beams. The length of the slit is along the Y direction and therefore the spatial separation of the mixing field due to momentum conservation can be determined along the Y direction of the CCD. The harmonic emission is dispersed along the X direction of the CCD. A collinear configuration of the two beams is applied for precise control of the time evolution of the output.

III.2. Wave-mixing with high-order harmonics in extreme ultraviolet region

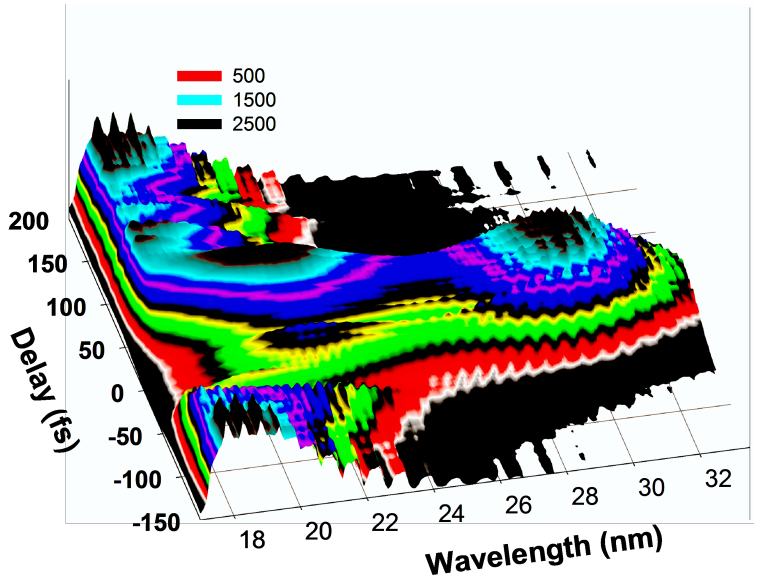

Fig. 1. Spatially integrated HHG spectrum generated by a 1400 nm driving pulse versus delay time of the 800 nm controlling pulse.

In this case the 800 nm beam is aligned at a very small angle ($< 10^{\circ}$) to the direction of the 1400 nm beam. The intensity of the 800 nm pulse is kept low. Fig. 1 shows the spatially integrated HHG spectrum versus delay time between the 1400 nm and 800 nm pulses in the far-field. High-order harmonic radiation is generated at wavelengths down to 16 nm when the 1400 nm driving pulse is applied. When the 800 nm pulse is absent or at very long delay times ($> \pm 200$ fs) we obtain phase-matched radiation [10, 13] with well-resolved odd harmonics and a good beam

profile along the propagation direction of the 1400 nm driving pulse. The total HHG intensity is a maximum when the focus of the 1400 nm beam is $\sim$ 1 mm inside the gas cell.

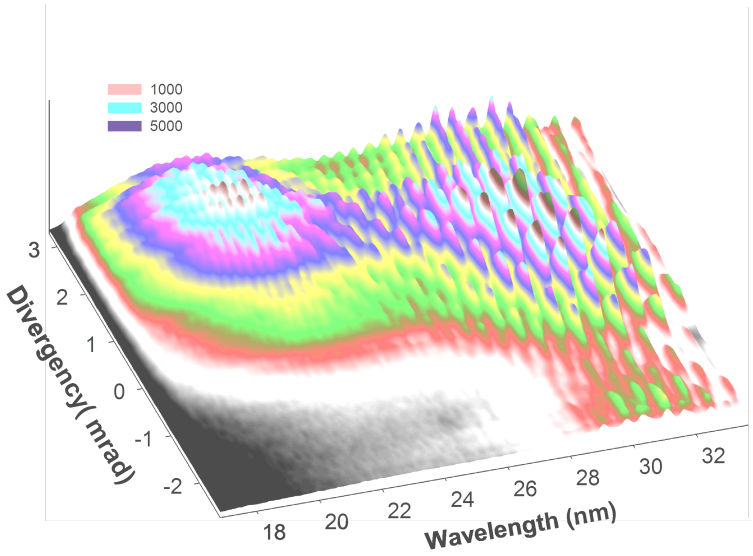

Fig. 2. HHG spectrum versus angular divergence for the focus plane of the spectrometer at a delay time of $\sim$ 10 fs between the 1400 nm and 800 nm pulses.

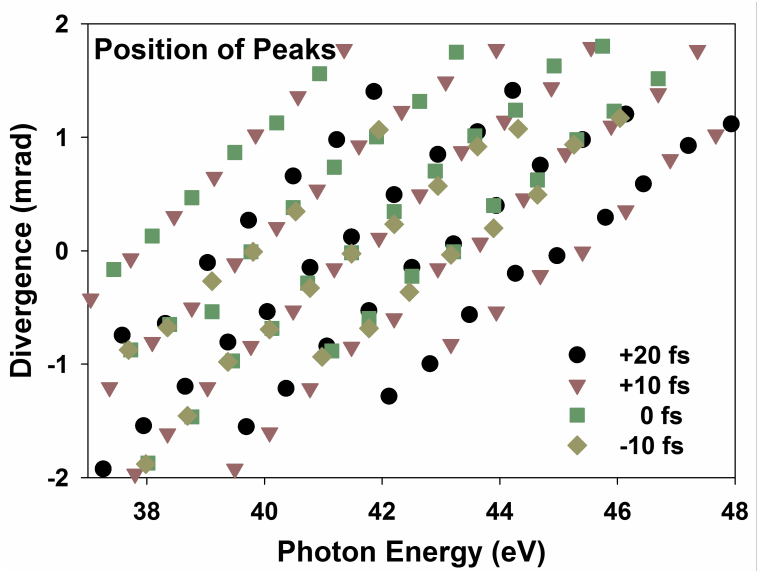

Fig. 3. Spatial and spectral position of the peaks in Fig. 2 for different delay times between the 1400 nm and 800 nm pulses.

The spectrum of the XUV radiation varies markedly with the influence of the second (800 nm) pulse. At zero delay between the two pulses a quasi-continuum XUV spectrum is obtained.

The addition of a second optical field whose frequency is not commensurate with that of the primary field creates additional frequency components in the HHG spectrum. The spectrum and spatial features, which are observed on the CCD, are modified with the delay time between the two pulses. For long delay times a Gaussian beam profile along the axis of the driving pulse is obtained, while for short delay times the beam profile consists of many clearly resolved peaks.

In Fig. 2 we show the spectrum versus divergence from the 1400 nm beam direction axis for a fixed time delay $\sim$ 10 fs, as an example. The discrete spatial and spectral peaks in the CCD image are caused by frequency mixing of the two fields - the harmonic field generated by the 1400 nm driving beam and the delayed 800 nm controlling field. The spectrum exhibits distinguishable peaks which indicate the position of the wave-mixing radiation. The spatial and spectral positions of the peaks vary with delay time between the two pulses as shown in Fig. 3. The spectral and spatial separation of the peaks is likely to be unchanged for a given delay. The 1400 nm beam alone generates a high-harmonic spectrum along the optical axis (divergence $\theta = 0$). The addition of the 800 nm field gives rise to off-axis radiation at different angles in the vertical Y direction. Conservation of energy and momentum for the generation of the resulting XUV emission need to be considered. To emit a single XUV photon, parity conservation requires that for a dipole transition the wave function of the continuum electron and the ion together must be in a state of different parity to that of the original ground state [7–9]. Therefore, only the net absorption of an odd total number of photons n = n_1 + n_2 can lead to photon emission. These selection rules can be written alternatively as: $\omega_q = n_1\omega_1 + n_2\omega_2$; $\boldsymbol{k}_q = n_1\boldsymbol{k}_1 + n_2\boldsymbol{k}_2$; $n_1 + n_2 = 2j+1$, where j is an integer, ω_1 is the carrier frequency of the 1400 nm field and ω_2 is the carrier frequency of the 800 nm field. From this approach, it is possible to produce a radiated frequency $\omega_q = (2j+1)\omega_1 \pm n(\omega_2 - \omega_1)$ and along directions $\boldsymbol{k}_q = (2j+1)\boldsymbol{k}_1 \pm n(\boldsymbol{k}_2 - \boldsymbol{k}_1)$ for various (j,n) combinations. The linear separation of the peaks (Fig. 3) confirms the requirement of perturbative optics.

For a detailed study of the time evolution of the mixing process the time difference of the two fields across the beam profile needs to be considered; therefore a collinear propagation of the two fields is used. In this configuration the time evolution of the mixing field is obtained with an error of < 1 fs, i.e., small compared with the optical cycle of the 800 nm field.

Figure 4 shows the spectrum of the XUV output versus delay time of the two beams. The time evolution for the different mixing fields can be analyzed in the wavelength range around 30 nm where the spectral resolution of the spectrometer is high. We measure the intensity of the mixing peak with high spectral resolution versus time delay of the 800 nm field. These results are shown in the inset of Fig. 4 for some mixing fields. For negative time delay the intensity of the mixing field increases rapidly and its profile is similar to that of the intensity of the laser pulses. For positive delay times the decay time is longer that the pulse duration and some oscillations of the mixing field's intensity can be observed. The decay time reflects the coherence time of the free electron wave-packet. It is interesting to see that the time evolution of the mixing field intensities is related to the intensity envelope of the laser field and we cannot see the high frequency (optical cycle) oscillation. The generation of high-order harmonics caused by the high intensity 1400 nm driving field is a nonperturbative process but it can be treated perturbatively for the mixing process with a second 800 nm second field.

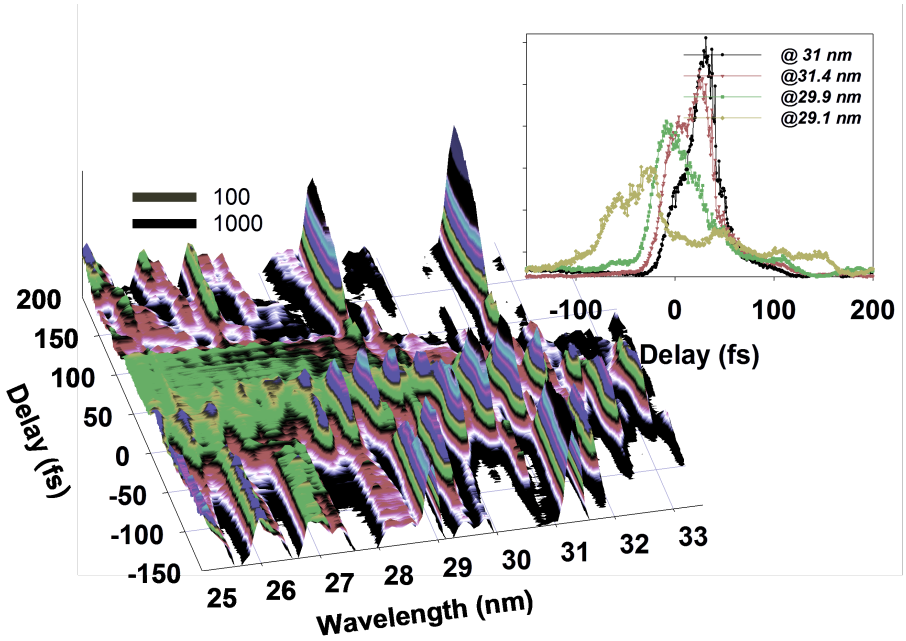

Fig. 4. HHG spectrum generated by a 1400 nm driving pulse versus delay time of the 800 nm controlling pulse in a co-propagating configuration. The inset shows the high spectral resolution of the radiation.

III.3. Perturbative Optical Parametric Amplification

The high-order harmonic radiation can be generated at wavelengths down to 16 nm when an 800 nm pulse, a 1400 nm pulse or both pulses together are used with argon gas at a pressure of 300 Torr. The spectrum of the HHG radiation generated by the intense 800 nm driving pulse is complex: not only odd orders but also even orders are generated and the beam profile is broad. The intensity of radiation below 20 nm is very weak. Because the intensity of the 800 nm pulse is $\geq 7.10^{14}$ W/cm^2 around the focus the ionization fraction is $\geq 15\%$ at the peak of the pump pulse which is much larger than the critical ionization fraction (3%) for phase-matched generation of high-order harmonics in an argon medium [11,12].

Figure 5 shows the variation of the XUV output spectrum versus delay time between the two pulses at 800 nm and 1400 nm. The separation of the focus position of the 800 nm and 1400 nm beams is $\sim$ 1 mm. For negative delay, the harmonic intensity increases with increasing delay time. A maximum of the total XUV radiation is obtained when the two pulses are at zero delay time. For a long delay < -100 fs the harmonic spectrum consists of odd harmonic orders of the 1400 nm pulse. For a short negative delay time < -40 fs other peaks can be seen between the odd orders of 1400 nm which are caused by frequency mixing with the 800 nm pulse [9]. The harmonic intensity decreases more rapidly on the positive delay side than on the negative delay side. This is caused by the high ionization rate created by the leading edge of the pump pulse which increases the phase-mismatch.

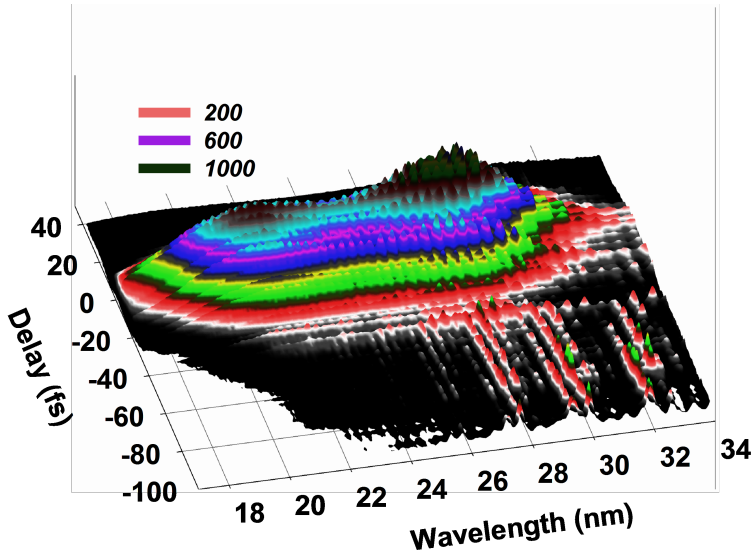

Fig. 5. Spectrum of XUV radiation along the optical axis of the pump pulse versus delay time between the 800 nm and 1400 nm pulses.

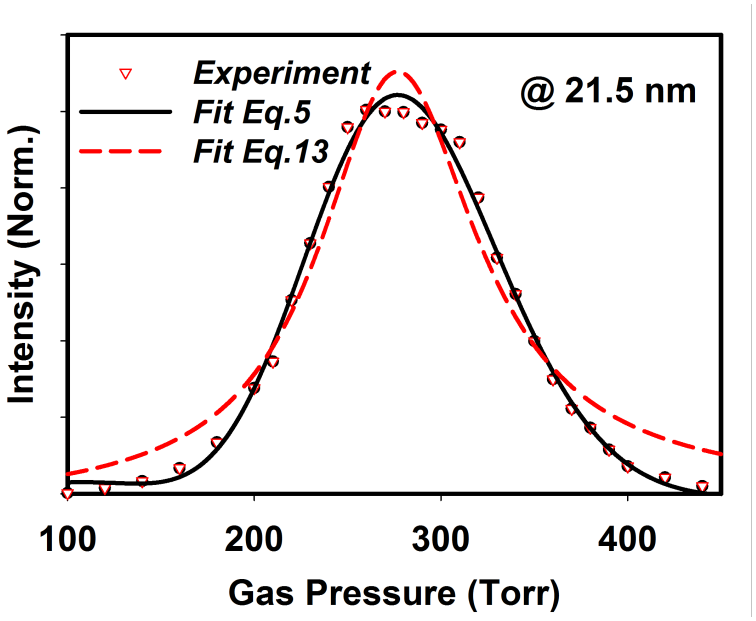

Fig. 6. Pressure dependence of XUV radiation for the case of the two pulses, 800 nm and 1400 nm, The experimental data (triangles) and the fit for amplification (solid line) and for phase-matched generation (dash line) is shown.

Figure 6 shows the variation of harmonic intensity for different pressures (100 to 450 Torr) of the medium. At low gas pressure phase-mismatch is small ($\Delta k \approx 0$). At high pressure the phase-mismatch is high and self-absorption of the medium plays an important role at pressures $>$ 350 nm.

When the high intensity 800 nm beam is used a good fit to the experimental data is obtained with Eq. (7), as shown by the solid line in Fig. 6. The measured yield increases exponentially with pressure in the range 150 to 250 Torr ($\Delta k \approx 0$) which reflects the amplification process. The phase-mismatch causes a decrease of the XUV intensity in the parametric amplifier and is large at high pressure. We note that the fit with the phase-matched generation process reflected by Eq. (14) (see Fig. 6, dash line) is not good at low and high pressure. With the amplification model, we are able not only to account for the XUV intensity but also to determine pump laser parameters such as the pump intensity and interaction length necessary for maximizing the gain.

IV. CONCLUSION

The combination of two laser fields with controllable intensity opens a new way for the generation and amplification of extreme ultraviolet radiation which is a step towards obtaining attosecond pulses with high intensity. We confirm that a perturbative formalism can be developed around the generation and amplification process, up to ultra-high orders of nonlinearity. A perturbative treatment in the high-order harmonic frequency region will help in the investigation of quantum effects in atoms and molecules in the high photon energy range.

REFERENCES

[1] N. Bloembergen and P. Pershan, *Physical Review* **128** (1962) 606.
[2] S. Mukamel, *Principles of nonlinear optical spectroscopy, 1995*, Oxford University Press, 1995.
[3] O. Smirnova, Y. Mairesse, S. Patchkovskii, N. Dudovich, D. Villeneuve, P. Corkum and M. Y. Ivanov, *Nature* **460** (2009) 972.
[4] H. Wörner, J. Bertrand, D. Kartashov, P. Corkum and D. Villeneuve, *Nature* **466** (2010) 604.
[5] J. Itatani, J. Levesque, D. Zeidler, H. Niikura, H. Pépin, J.-C. Kieffer, P. B. Corkum and D. M. Villeneuve, *Nature* **432** (2004) 867.
[6] H. Vu Le, K. Ba Dinh, P. Hannaford and L. Van Dao, *J. Appl. Phys.* **116** (2014) 173104.
[7] L. Dao, K. Dinh and P. Hannaford, *Appl. Phys. Lett.* **103** (2013) 141115.
[8] J. Bertrand, H. Wörner, H.-C. Bandulet, E. Bisson, M. Spanner, J.-C. Kieffer, D. Villeneuve and P. Corkum, *Phys. Rev. Lett.* **106** (2011) 023001.
[9] L. V. Dao, K. B. Dinh, H. V. Le, N. Gaffney and P. Hannaford, *App. Phys. Lett.* **106** (2015) 021118.
[10] L. Dao, K. B. Dinh and P. Hannaford, *Nat. Commun.* **6** (2015) 7175.
[11] S. Meyer, B. Chichkov, B. Wellegehausen and A. Sanpera, *Phys. Rev. A* **61** (2000) 063811.
[12] T. Popmintchev, M.-C. Chen, O. Cohen, M. E. Grisham, J. J. Rocca, M. M. Murnane and H. C. Kapteyn, *Opt. Lett.* **33** (2008) 2128.
[13] L. V. Dao, C. Hall, H. L. Vu, K. B. Dinh, E. Balaur, P. Hannaford and T. A. Smith, *Applied optics* **51** (2012) 4240.